# High thermoelectric power factor from multilayer solution-processed organic films

Guangzheng Zuo, Olof Andersson, Hassan Abdalla and Martijn Kemerink


Zuo, G., Andersson, O., Abdalla, H., Kemerink, M., (2018), High thermoelectric power factor from multilayer solution-processed organic films, *Applied Physics Letters*, 112(8), 083303.
https://doi.org/10.1063/1.5016908

# High Thermoelectric Power Factor from Multilayer Solution-Processed Organic Films

Guangzheng Zuo, Olof Andersson, Hassan Abdalla and Martijn Kemerink *

Complex Materials and Devices, Department of Physics, Chemistry and Biology (IFM), Linköping University, 58183 Linköping, Sweden

E-mail: martijn.kemerink@liu.se

## Abstract

We investigate the suitability of the 'sequential doping' method of organic semiconductors for thermoelectric applications. The method consists of depositing a dopant ($F_4TCNQ$) containing solution on a previously cast semiconductor (P3HT) thin film to achieve high conductivity, while preserving the morphology. For very thin films (~25 nm) we achieve a high power factor around 8 $\mu W/m \cdot K^{-2}$ with a conductivity over 500 S/m. For increasing film thickness conductivity and power factor show a decreasing trend, which we attribute to the inability to dope the deeper parts of the film. Since thick films are required to extract significant power from thermoelectric generators, we developed a simple additive technique that allows the deposition of an arbitrary number of layers without significant loss in conductivity or power factor that, for 5 subsequent layers, remain at ~300 S/m and ~5 $\mu W/m \cdot K^{-2}$, respectively, whereas the power output increases almost one order of magnitude as compared to a single layer. The efficient doping in multilayers is further confirmed by an increased intensity of (bi)polaronic features in the UV-Vis spectra.

Keywords: Seebeck coefficient; organic thermoelectrics; $F_4TCNQ$; doping; processing

The thermoelectric effect turns a temperature difference directly into electricity. To use this to harvest e.g. waste heat with an efficiency that approaches the Carnot efficiency, the thermoelectric material needs a high, preferably larger than unity, figure of merit $ZT = \sigma S^2/\kappa T$, with $\sigma$ the conductivity, $S$ the Seebeck coefficient and $\kappa$ the thermal conductivity. Organic semiconductors are widely used in LEDs, solar cells, field-effect transistors and so on [1–4] and are receiving increasing attention for thermoelectric applications, largely driven by an inherently low $\kappa$ and a relatively high $S$ as well as by the promise of compatibility with cheap, large-area production.[5,6] Indeed, PEDOT-based materials can achieve $ZT$ around 0.25[7] but most other organic thermoelectric materials perform significantly worse because of a low conductivity.

Molecular doping is an effective way to increase the conductivity of organic semiconductors[8–10]. Over the years, P3HT doped by $F_4$TCNQ has become the field's fruit fly system, and the doping mechanism and kinetics have been researched by several groups[11–15]. In conventional solution processing the doped layer is deposited from a common solution containing both the semiconductor (P3HT) and the dopant ($F_4$TCNQ) – in the following we shall refer to this as bulk doping. Using this method one can get a conductivity of doped P3HT around $4\times10^{-2}$ S/m and a power factor $PF = \sigma S^2$ around $6\times10^{-3}$ μW/m·K$^{-2}$[16]. A major problem with the bulk doping method is that the large amount of $F_4$TCNQ negatively affects the morphology of the P3HT film, and leads to $F_4$TCNQ aggregation, preventing one to achieve higher conductivity[17,18]. Müller's group has shown that adding PEO to the solution of P3HT with $F_4$TCNQ increases the stability of the solution, achieving a conductivity for the ternary system of ~30 S/m and a power factor ~0.1 μW/m·K$^{-2}$ [19].

Another issue that has to be addressed to make relevant organic thermoelectric generators is the thickness of the active layer that has to be increased to at least the μm regime to obtain significant absolute power outputs[19,20]. Recently, Hwang et al. reported on a sequential deposition-doping procedure leading to μm-thick films of $Fe^{3+}$-$tos_3$·$6H_2O$-doped P3HT with a high conductivity around $5.5\times10^3$ S/m and a record power factor around 30 μW/m·K$^{-2}$[20]. Unfortunately, the method requires extended (~1 hr) submerging of the P3HT film in dopant solution and gave less satisfying results for the weaker oxidant $F_4$TCNQ. Patel et al. showed that PBTTT vapor-doped with $F_4$TCNQ on OTS-treated substrates can give a high power factor around 120 μW/m·K$^{-2}$, but the active layer thickness was just ~25 nm, which limits the absolute power output[21].

Here, we aim to overcome the drawbacks of bulk doping of P3HT with $F_4$TCNQ using a 'fast' solution processing method. To this end, we adopt a simple, recently proposed method of sequential 'surface doping' by spin-coating dopant solution over an already cast P3HT film[22]. Scholes et al. have shown that this procedure can achieve high conductivity (~$5.5\times10^2$ S/m) by preserving the film morphology. Using this surface doping method, we arrive at similar conductivities as Scholes et al. and at a power factor ~8 μW/m·K$^{-2}$ for thin (<100 nm) films. Films with μm thickness and similar

doping efficiency, conductivity and power factor can be made by alternate deposition of semiconductor and doping layers. As an example, we made a 5-layer micro-film with conductivity and power factor of ~$3\times10^2$ S/m and ~5 μW/m·K$^{-2}$, respectively. The latter is the highest so far reported value for $F_4$TCNQ-doped P3HT. The simple layer-by-layer (LbL) method explored here has a different goal than usual, in that we target homogeneous films of increased thickness instead of the heterogeneous multilayers that are targeted when LbL methods are used for the assembly of nanocomposite materials.[23] The latter has e.g. been used by Grunlan et al. in the fabrication of complex organic multilayers for thermoelectric applications.[24,25]

The fabrication procedures of single and multi-layer devices are illustrated in Fig. 1. In both cases, semiconductor (P3HT) and dopant ($F_4$TCNQ) were sequentially deposited by spin coating from separate solutions on either the clean substrate or the previous layer. The conductivity and Seebeck coefficient measurements were performed using a 4-point probe setup in a glove box under nitrogen atmosphere at room temperature. Further experimental details can be found in the Supplementary Material (SM).

Single P3HT layers with a range of thicknesses from 25 nm to 500 nm were prepared and subsequently surface doped by $F_4$TCNQ to investigate the effect of thickness on conductivity, Seebeck coefficient and power factor. The results are shown in Fig. 2. For the thinnest films, we find a conductivity ~$6\times10^2$ S/m and a Seebeck coefficient ~120 μV/K combining into a high PF over 8 μW/m·K$^{-2}$ at 25 nm – previously, PFs around $10^{-3}$ – $10^{-1}$ μW/m·K$^{-2}$ were reported for the same material combination using bulk doping[16,19]. Although obtaining record values was not the purpose of this work (e.g. the $F_4$TCNQ concentration was not varied/optimized), our results compare favorably to previous literature values, as shown in the SM. The high conductivity numbers we find for thin films are in good agreement with earlier work, suggesting that indeed the ordered morphology of P3HT is not negatively affected by the surface doping procedure and that similar charge carrier concentrations around $4\times10^{26}$ m$^{-3}$ have been obtained for the thinnest films.[22] This is further corroborated by the atomic force microscopy (AFM) images shown in Fig. 3a, b that show no visible effects of the $F_4$TCNQ deposition on the surface topography. The pure P3HT film shows a smooth morphology with a roughness $R_q$ = 0.92 nm; after spin-coating a single layer of $F_4$TCNQ this becomes $R_q$ = 0.82 nm.

For thicker films, we find that the conductivity decreases significantly while the Seebeck coefficient slightly increases. Both factors imply that the overall doping efficiency goes down with increasing thickness. In line with the recent work by Kolesov et al.[26], we attribute this to the dopant not managing to penetrate more than a certain depth, leaving any deeper parts of thicker films less doped or undoped. In the thickness range 25–150 nm the conductivity seems to first go down, followed by an upturn before continuing the overall decreasing trend. The local minimum at ~75 nm is also reflected in the Seebeck coefficient and the trend has been reproduced between samples made on different days from

different stock solutions. Although providing an elaborate explanation for the non-monotonous behavior is beyond the main purpose of the present work, we can speculate that it is related to an interplay between the thickness dependence of the P3HT morphology and the decreasing doping concentration with increasing thickness. Recently, Huang et al. found a strong thickness dependence of the anisotropy of rr-P3HT; specifically, between ~5 and ~100 nm the fraction of (substrate-induced) edge-on crystals was found to decay strongly.[27] Hence, we attribute the first drop in in-plane conductivity to a reduced π-π stacking in the current direction. The upturn and subsequent second decay of the conductivity is attributed to the (decaying) mean doping concentration passing through an optimal value. Since chemical doping has both a beneficial effect on the mobility, through state filling, as well as a detrimental effect, through Coulomb scattering by ionized dopants and possibly some morphology degradation,[14] one may anticipate an optimal thickness at which the concentration (profile) is optimal. Note also that for the whole thickness range 25–150 nm o-DCB was used so effects of a change of solvent to CF (>200 nm) can be ruled out.

We checked whether additional $F_4TCNQ$ depositions would lead to a higher conductivity and fabricated devices with 3 spin-coated dopant layers on a single, 150, 340 or 500 nm thick P3HT film. Somewhat surprisingly, we did not observe significant increases in conductivity, as shown by the yellow dots in Fig. 2. This suggest that the surface doping process is self-limiting in that the relatively small dopant molecules fill the pores in the swollen polymer film, blocking further penetration on the time scale of the surface doping process. In case of diffusion-limited doping, extending the diffusion time by subsequent doping steps would lead to a gradual increase in conductivity for the thicker samples which is not observed. The sketched scenario would be consistent with the very minor changes in surface morphology of the triple-doped film ($R_q$ = 1.15 nm) as shown in Fig. 3c that also shows that no large amounts of $F_4TCNQ$ remain on the film surface after multiple depositions. If this were the case, the topography would rather resemble that of pure $F_4TCNQ$ as shown in Fig. 3d.

From the above, it seems impossible to increase the film thickness of single-layer devices without suffering significant PF losses. Therefore, we turned to the idea of building multi-layer devices by alternate deposition of (thin) semiconductor and dopant layers, as illustrated in Fig.1. We anticipated that the $F_4TCNQ$-enriched top layer would prevent dissolution and/or delamination of already deposited layers upon additional spin coating steps. Indeed, the thickness of sequentially doped P3HT films is constant within experimental uncertainty upon spin-coating pure o-DCB solvent on top, even if the procedure was repeated up to 5 times, while pure P3HT films were dissolved by the same procedure. The conductivity of the surface doped films gradually decreased to about one third of the initial value after 3 or more rounds of o-DCB deposition. We attribute this decrease to some part of $F_4TCNQ$ molecules being removed from the doped P3HT film by the solvent.

To evaluate possible differences in doping efficiency upon deposition of multiple layers of sequentially doped P3HT, we performed UV-Vis spectroscopy on pristine and doped single and double layers as shown in Fig. 4. Firstly, we checked the difference between pure and doped P3HT (single layer) films. In line with literature we found that the doped P3HT has a strong and broad absorption between 650 nm 1100 nm, whereas no absorption in this region is seen for the pure P3HT film. The two peaks around 770 nm and 850 nm indicate the presence of (bi)polarons in the doped film[28,29]. The UV-Vis spectrum of the double layer film shows significantly stronger absorption peaks at 770 nm and 850 nm, which suggests a larger doping efficiency in double layers, likely due to dopant molecules also diffusing in from the bottom upon deposition of the second semiconductor layer – Fig. S5 in the SM shows that this indeed happens. Similar measurements on triple and higher multi layers became inconclusive due to the films getting completely absorbing.

Next, the performance of multilayer devices was investigated, and the results are shown in Fig. 5a. We find that $\sigma$, $S$ and $PF$ are almost constant when going from 1 to 5 layers, with $\sigma$ over 300 S/m and PF close to 5 µW/m·K$^{-2}$. To illustrate the contrast between an active layer consisting of a thick single layer and one consisting of multiple thinner layers, Fig. 5b shows the device current at zero temperature difference $\Delta T$ between the contacts as a measure of the device conductance and the output power at $\Delta T$ = 1 K. The power output is estimated by $P = \mathrm{PF}\Delta T^2 A/l$ where the area $A = wt$ with $w$ the width of the contacts (7 mm), $t$ the film thickness and $l$ the channel length (5 mm). Fig. 5b shows both the current and the power output increase by an order of magnitude in going from 1 to 5 layers, in stark contrast to single-layer devices of increasing thickness, which decrease dramatically in $PF$. For the scalability of the method it is important that the increases in current and power are close to linear as shown by the trendline in Fig. 5b. We attribute the larger thickness of successive layers than that of the first layer to the different underlayer (doped P3HT vs. glass).

While we have shown that our method can deposit several hundreds of nm of material per deposition round without significant loss in thermoelectric performance, deposition of mm thick layers as would be needed for conventional out-of-plane thermoelectric generators would require an unpractically high number of depositions. However, the flexibility of organic thermoelectrics allows to fold or roll much thinner 2D layers into 3D architectures. For such 2D in-plane elements, layer thicknesses in the µm range are relevant.[6] Our used (spin coating) deposition technique is evidently not scalable to larger areas but it is realistic to assume that the methodology is. The complete absence of delamination problems should enable a rather straightforward transfer to typical low-cost processing approaches like slot-dye coating or ink-jet printing.

In conclusion, we have developed a simple and scalable method to deposit µm thick films of a prototypical doped polymer semiconductor (P3HT p-type doped by $F_4$TCNQ) for thermoelectric applications. We employed sequential doping to reach high doping concentrations without

significantly sacrificing morphology. As the effectiveness of the doping step became less for increasing layer thickness, thicker films were deposited by alternating depositions of the semiconductor and the dopant, yielding a virtually linear scaling of device conductance and thermoelectric output power with layer thickness. For thin (< ~150 nm) single-layer films, a conductivity over 400 S/m and a high power factor around 7 $\mu W/m \cdot K^{-2}$ were obtained, shifting to 300 S/m and 5 $\mu W/m \cdot K^{-2}$ for thick (>1 µm) multilayer films.

**Supplementary Material**

See the Supplementary Material for experimental details regarding device fabrication, electric and thermoelectric characterization, the (absence of) contact resistance and a comparison to previously reported thermoelectric performance indicators.

**Acknowledgements**:

The research by GZ is supported by the China Scholarship Council (CSC). O.A. and H.A. gratefully acknowledge funding by the Knut och Alice Wallenbergs stiftelse (project ‘Tail of the Sun’). We are grateful to Indrė Urbanavičiūtė for help with the AFM measurements, and Xianjie Liu for useful discussions.

## References


[1] X. Zhou, J. Blochwitz, M. Pfeiffer, A. Nollau, T. Fritz, and K. Leo, Adv. Funct. Mater. **11**, 310 (2001).
[2] H. Zhou, L. Yang, and W. You, Macromolecules **45**, 607 (2012).
[3] O. Bubnova and X. Crispin, Energy Environ. Sci. **5**, 9345 (2012).
[4] S. Kola, J. Sinha, and H.E. Katz, J. Polym. Sci. Part B Polym. Phys. **50**, 1090 (2012).
[5] Q. Zhang, Y. Sun, W. Xu, and D. Zhu, Adv. Mater. **26**, 6829 (2014).
[6] B. Russ, A. Glaudell, J.J. Urban, M.L. Chabinyc, and R.A. Segalman, Nat. Rev. Mater. **1**, natrevmats201650 (2016).
[7] O. Bubnova, Z.U. Khan, A. Malti, S. Braun, M. Fahlman, M. Berggren, and X. Crispin, Nat. Mater. **10**, 429 (2011).
[8] A.M. Glaudell, J.E. Cochran, S.N. Patel, and M.L. Chabinyc, Adv. Energy Mater. **5**, n/a (2015).
[9] P. Wei, J.H. Oh, G. Dong, and Z. Bao, J. Am. Chem. Soc. **132**, 8852 (2010).
[10] P. Pingel, R. Schwarzl, and D. Neher, Appl. Phys. Lett. **100**, 143303 (2012).
[11] V.I. Arkhipov, E.V. Emelianova, P. Heremans, and H. Bässler, Phys. Rev. B **72**, 235202 (2005).
[12] Y. Zhang, H. Zhou, J. Seifter, L. Ying, A. Mikhailovsky, A.J. Heeger, G.C. Bazan, and T.-Q. Nguyen, Adv. Mater. **25**, 7038 (2013).
[13] P. Pingel and D. Neher, Phys. Rev. B **87**, 115209 (2013).
[14] G. Zuo, H. Abdalla, and M. Kemerink, Phys. Rev. B **93**, 235203 (2016).
[15] F.M. McFarland, L.R. Bonnette, E.A. Acres, and S. Guo, J. Mater. Chem. C **5**, 5764 (2017).
[16] J. Sun, M.-L. Yeh, B.J. Jung, B. Zhang, J. Feser, A. Majumdar, and H.E. Katz, Macromolecules **43**, 2897 (2010).
[17] D.T. Duong, C. Wang, E. Antono, M.F. Toney, and A. Salleo, Org. Electron. **14**, 1330 (2013).
[18] G. Zuo, Z. Li, O. Andersson, H. Abdalla, E. Wang, and M. Kemerink, J. Phys. Chem. C **121**, 7767 (2017).
[19] D. Kiefer, L. Yu, E. Fransson, A. Gómez, D. Primetzhofer, A. Amassian, M. Campoy-Quiles, and C. Müller, Adv. Sci. **4**, n/a (2017).
[20] S. Hwang, W.J. Potscavage, R. Nakamichi, and C. Adachi, Org. Electron. **31**, 31 (2016).
[21] S.N. Patel, A.M. Glaudell, K.A. Peterson, E.M. Thomas, K.A. O'Hara, E. Lim, and M.L. Chabinyc, Sci. Adv. **3**, e1700434 (2017).
[22] D.T. Scholes, S.A. Hawks, P.Y. Yee, H. Wu, J.R. Lindemuth, S.H. Tolbert, and B.J. Schwartz, J. Phys. Chem. Lett. **6**, 4786 (2015).
[23] G. Decher and J.B. Schlenoff, editors , in *Multilayer Thin Films* (Wiley-VCH Verlag GmbH & Co. KGaA, 2012), pp. i–XXIV.
[24] C. Cho, B. Stevens, J.-H. Hsu, R. Bureau, D.A. Hagen, O. Regev, C. Yu, and J.C. Grunlan, Adv. Mater. **27**, 2996 (2015).
[25] C. Cho, K.L. Wallace, P. Tzeng, J.-H. Hsu, C. Yu, and J.C. Grunlan, Adv. Energy Mater. **6**, n/a (2016).
[26] V.A. Kolesov, C. Fuentes-Hernandez, W.-F. Chou, N. Aizawa, F.A. Larrain, M. Wang, A. Perrotta, S. Choi, S. Graham, G.C. Bazan, T.-Q. Nguyen, S.R. Marder, and B. Kippelen, Nat. Mater. **16**, 474 (2017).
[27] B. Huang, E. Glynos, B. Frieberg, H. Yang, and P.F. Green, ACS Appl. Mater. Interfaces **4**, 5204 (2012).
[28] C. Wang, D.T. Duong, K. Vandewal, J. Rivnay, and A. Salleo, Phys. Rev. B **91**, 085205 (2015).
[29] H. Méndez, G. Heimel, S. Winkler, J. Frisch, A. Opitz, K. Sauer, B. Wegner, M. Oehzelt, C. Röthel, S. Duhm, D. Többens, N. Koch, and I. Salzmann, Nat. Commun. **6**, ncomms9560 (2015).

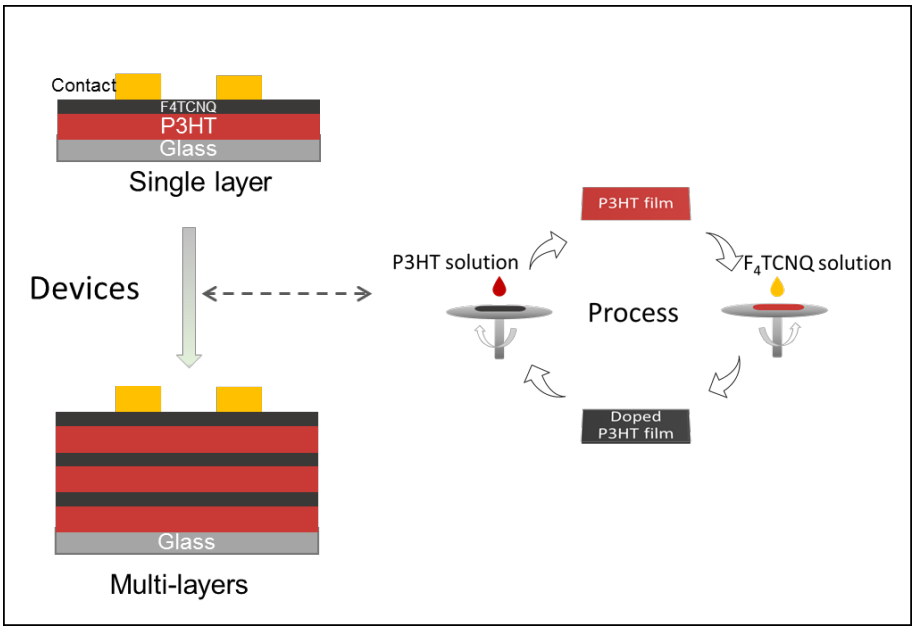


FIG. 1 Schematic of the sample structure and of the applied process to fabricate single and multilayer devices.

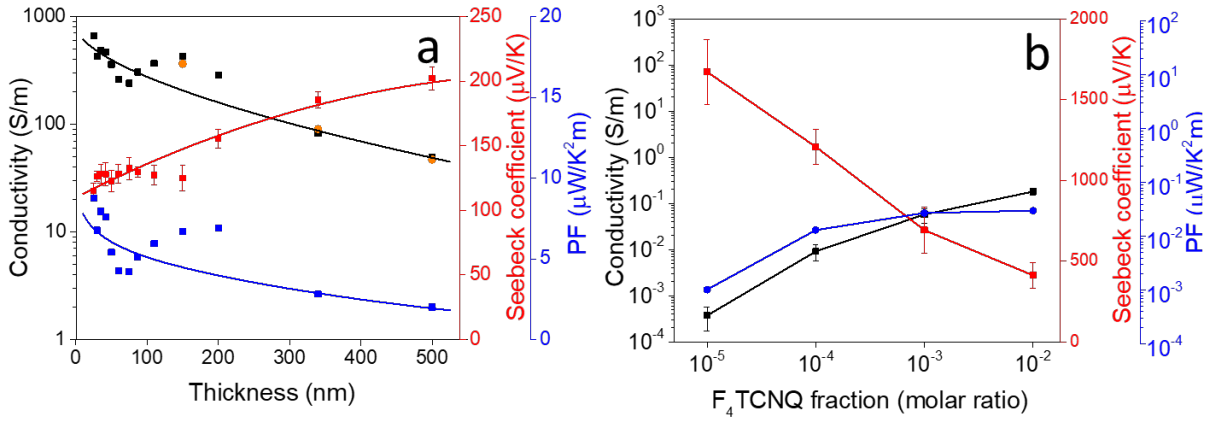


FIG. 2 Conductivity, Seebeck coefficient and power factor vs. thickness from single layer devices. Orange dots indicate the conductivity of samples of which the P3HT film has been surface doped by 3 successive $F_4TCNQ$ layers. Gray squares show conductivities from bulk-doped P3HT with $F_4TCNQ$ from $10^{-5}$ to$10^{-2}$ molar ratio at ~150 nm. Data points are averages over multiple devices, the error bar on the conductivity is smaller than the symbol size. Lines are guides to the eye.

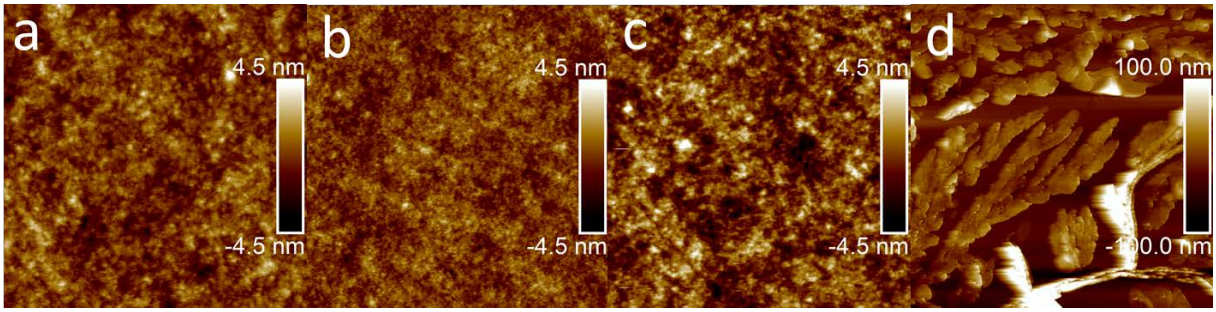


FIG. 3 AFM height images for pure P3HT (a), pure $F_4TCNQ$ (d) and surface doped P3HT with 1 (b) and 3 (c) spin-coated $F_4TCNQ$ layers. The scan size is 2×2 µm in a-c and 20×20µm in d;

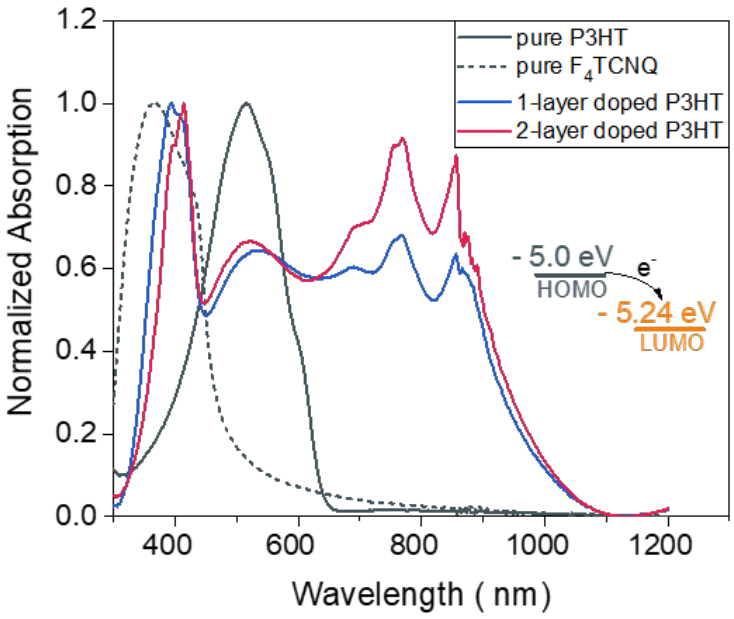


FIG. 4 Normalized UV-Vis absorption spectra for thin films of pure $F_4TCNQ$ and P3HT, and for single and double layers of $F_4TCNQ$-doped P3HT as specified in the legend. The inset shows the integer charge transfer between the P3HT HOMO (-5.0 eV) and the $F_4TCNQ$ LUMO (-5.24 eV)

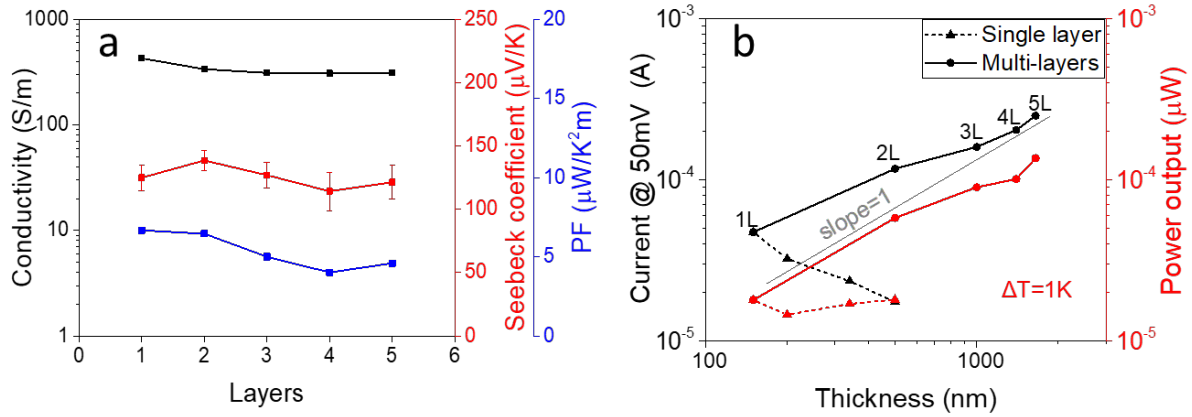


FIG. 5 (a) Conductivity, Seebeck coefficient and power factor vs. number of deposited P3HT:$F_4$TCNQ layers; (b) current at 50 mV and estimated power output at $\Delta T$ = 1 K (solid line + circles: multilayer; dashed line + triangles: single- layer), vs. layer thickness. Data points are averages over multiple devices, the error bar on the conductivity is smaller than the symbol size.